



Ecological indication based on source, content, and structure characteristics of dissolved organic matter in surface sediment from Dagu River estuary, China

Maomao Li¹ · Fanlong Kong¹ · Yue Li¹ · Junlong Zhang^{1,2}  · Min Xi¹

Received: 28 November 2019 / Accepted: 10 August 2020 / Published online: 14 August 2020
© Springer-Verlag GmbH Germany, part of Springer Nature 2020

Abstract

Dissolved organic matter (DOM) controls the fate of a variety of nutrients and trace metals in river estuary systems. The aim of our study is to explore the sources, structure characteristics of sediment DOM, and potential ecological release risk (heavy metal, N and P) under the environmental conditions of Dagu River estuary. The relative contribution of DOM source was calculated by carbon stable isotope (combining $\delta^{13}\text{C}_{\text{DOM}}$ and C/N ratios). The structural characteristics of sediment DOM in Dagu River estuary were determined by ultraviolet-visible spectroscopy (UV-vis) absorbance and fluorescence spectroscopy. The potential ecological risks of heavy metals and N and P release were also assessed. Results show that the relative contributions of rural area and aquaculture are high in Dagu River estuary. The humification degree of DOM in downstream river is higher than that in the estuary, and the sediment DOM in Dagu River estuary is influenced by both terrestrial input and biological metabolism. The potential risk of eutrophication in the estuary is high. Moreover, under the effect of aquaculture and rural area, there is higher potential ecological release risk of heavy metal in the estuary. And samples in the middle transect have the highest potential ecological risks of heavy metal. Therefore, a framework has been proposed to predict the ecological status of the estuary by analyzing the sources, content, and structural characteristics of sediment DOM. These results provide a new insight on ecological indication of DOM in Dagu River estuary.

Keywords Dagu River · Sediment · Ecological risk · Dissolved organic matter · Estuary

Introduction

Estuaries, the transitional interface between freshwater and seawater, are significant regions where the continuous exchange of water and chemical components occur (Liu et al. 2018; Xie et al. 2018). Rapid population growth and industrial development lead to the environmental pollution and ecological deterioration in estuary systems. Some pollutants can

result in deleterious effect to the marine lives and possible poisoning to the human health (Jiang et al. 2017; Jahan and Strezov 2018). The fate of pollutants in estuary systems is related to the content and structural characteristics of dissolved organic matter (DOM) (Jiang et al. 2017). This is because DOM can alter metal speciation and transportation by absorbing and creating complexes with heavy metals (Louis et al. 2014). Besides, DOM can affect the content of nitrogen and phosphorus by a variety of biogeochemical processes due to its content and structural characteristics (Li et al. 2014).

The content and structural characteristics of DOM can be influenced by different sources (Guéguen et al. 2012; Shang et al. 2018). Previous studies showed that allochthonous DOM sources, such as industry, urban area, and agriculture practices, changed the content and composition of DOM in aquatic environment (Boyes and Elliott 2006; Cao et al. 2018; Zhang et al. 2020). For instance, Meng et al. (2013) found that the protein-like components of DOM are related to sewage inputs and microbial activity in streams. Hongve (1999) presented that the forest is an important contributor to DOM

Responsible Editor: Vedula VSS Sarma

✉ Junlong Zhang
zjunlong1021@126.com

✉ Min Xi
ximin@qdu.edu.cn

¹ College of Environmental Science and Engineering, Qingdao University, Qingdao 266071, Shandong, China

² Shandong Key Laboratory of Water Pollution Control and Resource Reuse, School of Environmental Science and Engineering, Shandong University, Jinan 250100, China

contents. Besides, sediments are ecologically important components of the estuary systems and important sources and sinks of DOM in water (Li et al. 2016; Omar et al. 2018). Sediment DOM has been widely studied, but previous studies mainly focused on its source, distribution, structure, DOC contents, and the reaction mechanism of DOM with pollutants, separately (Jiang et al. 2008; Huguet et al. 2010; Wang et al. 2015; Niu et al. 2017; Derrien et al. 2018; He et al. 2019; Zhang et al. 2019). The relationship between the source, characteristics of DOM, and the potential ecological risk (release of heavy metal and N, P) has rarely been addressed. In fact, there is a close connection between them. For instance, Li et al. (2014) disclosed that the contents and structural characteristics of sediment DOM, which are closely correlated with the sources, can affect the contents of DON. Li et al. (2016) indicated that high content of sediment DOM is related to high contents of DOP, DON, TN, and TDN in Dongting Lake.

Previous studies of DOM were mostly on rivers, catchments, lakes, and high-mountain glacial areas (Cong et al. 2015; Ji et al. 2015; Chen et al. 2017; Gul et al. 2018; Niu et al. 2018; Kang et al. 2019; Liu et al. 2019). To date, few studies have been performed on sediment DOM in the estuary. In fact, the characteristics of sediment DOM are likely to vary along the freshwater to the estuary area due to different major sources and environment conditions (Chen and Hur 2015). For instance, when the ocean is more aliphatic, terrestrial-derived DOM from freshwater tends to be more aromatic (Coble 1996; McKnight et al. 2001). This may cause differences in reactivities of DOM in the sediment of downstream river and estuaries. Therefore, it is important to study the relationship between source, structural characteristics, and reactivities of DOM for providing a better insight into ecological risk in estuary systems.

The analysis techniques for analyzing DOM have advanced over the last few decades (Leenheer and Croué 2003). Ultraviolet-visible spectroscopy (UV-vis) has been frequently applied to explore the characteristics of aromatic or unsaturated compound (Sellami et al. 2008). The three-dimensional excitation-emission matrix (3D-EEM) fluorescence spectrum is applied to detect the organic compounds which have the fluorescent characteristics (Tian et al. 2012; Zhu et al. 2020). The 3D-EEM also can provide lots of information about biogeochemical cycle and DOM composition (Wang et al. 2009). Besides, fluorescence regional integration (FRI) can be used for quantitative detection of EEM spectra by integrating volumes below various excitation-emission regions in the EEM spectrum (Chen et al. 2003; He et al. 2011; Li et al. 2014). The techniques above provide important tools for studies of structural characteristics of DOM (Xie et al. 2012; Li et al. 2015). In addition, Wu et al. (2012a) examined the sources of DOM utilizing the values of $\delta^{13}\text{C}$ and C/N ratio measurements. Thus,

we determine the sources of sediment DOM on the basis of the $\delta^{13}\text{C}_{\text{DOM}}$ and C/N ratios.

Dagu River estuary is strongly impacted by anthropogenic activities because of DOM inputs (Xi et al. 2017, 2018). And the anthropogenic activities have been leading to heavy metal pollution and eutrophication in coastal zone and offshore in recent years (Dai et al. 2007). Thus, the aims for our study were to (i) estimate source contribution of Dagu River estuary by isotope labeling quantitatively, and assess the impact of different land use types (human activities) on DOM structure characteristics; (ii) investigate the sediment DOM structural characteristics of Dagu River estuary by UV-vis spectroscopy and 3D-EEM spectroscopy; and (iii) assess the potential ecological risks of heavy metals and eutrophication based on DOM characteristics.

Materials and methods

Description of the study area

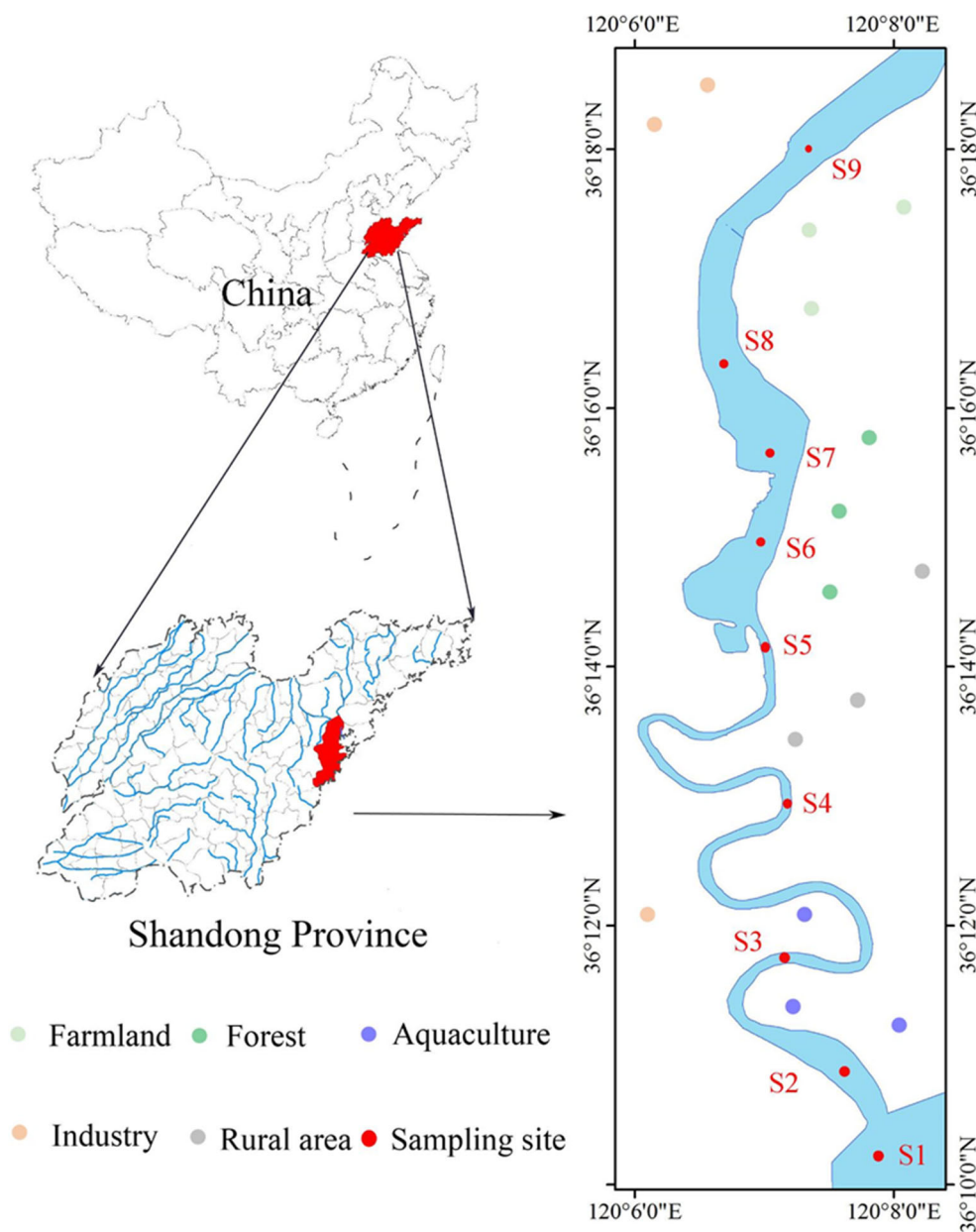
Jiaozhou Bay (36° 01'–36° 15' N, 120° 03'–120° 25' E), a typical semi-enclosed bay, is located on the south bank of the Shandong Peninsula, China. The coast of Jiaozhou Bay features a typical regular semi-diurnal tide. More than ten rivers drain into Jiaozhou Bay with various water loads. These are all seasonal rivers, with a dry season from February to May and a flood season from June to September. Dagu River, which has an annual average water runoff of 0.5 km³, is the largest among these rivers empty into Jiaozhou Bay, accounting for about 85.6% of total flow of other rivers (Xi et al. 2018) (Fig. 1).

Sample collection and treatment

Surface sediments (0–2-cm depth) were obtained from Dagu River estuary (S1–S9) in January, 2019. We divided the sampling sites into estuary, middle zone, and downstream river according to the distance from the sea. We called S1–S3 (which are near the sea) the estuary. S4–S6 are the middle zone, and S7–S9 (which are far from the sea) are the downstream river. Source samples of surface sediments (aquaculture pond), creeks (rural and industrial area), and surface soils (farmland and forest) were collected along Dagu River. The sampling area covered an area of 36° 10' 12.92" N to 36° 18' 26.53" N and 120° 5' 19.02" E to 120° 9' 59.62" E. After sampling, samples were put into polyethylene bags immediately, sealed, and transported to the laboratory. All samples were naturally dried, grinded, and selected through a 100-mesh sieve for further analysis (Dong et al. 2020).

Sediment DOM was extracted with Milli-Q water in soil-water slurry at a ratio of 1:5, and kept in a shaking bath (180 r/min) at room temperature for 30 min (Yu et al. 2019). Then

Fig. 1 Study area and sampling sites



the samples were centrifuged at 4000 r/min for 20 min. The clear supernatant was extracted and was filtered through 0.45- μm polyethersulfone membrane. The dissolved organic carbon (DOC) content was measured by KMnO_4 chromatometry method (Yu et al. 2019). The contents of $\text{NH}_4^+\text{-N}$, $\text{NO}_3^-\text{-N}$, TN, and available phosphorus (AP) in the sediment were also measured in this study.

Carbon stable isotope ratios ($\delta^{13}\text{C}_{\text{DOM}}$)

Before carbon stable isotope analysis, inorganic carbon was removed by 0.1 mol/L HCl treatment. Samples were analyzed in the lab using an isotope ratio mass spectrometer (precision of 0.15‰ for $\delta^{13}\text{C}$) and the isotopic results are given in the

standard δ notation. Stable isotope ratio δ is expressed as the deviation from standard in parts per thousand (‰) with the equation:

$$X(\text{‰}) = ((R_{\text{sample}}/R_{\text{reference}})-1) \times 1000 \quad (1)$$

where R_{sample} refers to the $^{13}\text{C}/^{12}\text{C}$ ratios for the sample, $R_{\text{reference}}$ refers to the $^{13}\text{C}/^{12}\text{C}$ ratios for the standard, and $X = \delta^{13}\text{C}_{\text{DOM}}$. Isotopic data are based on the international Vienna Pee Dee Belemnite (PDB) standard.

UV-vis, EEM measurements, and FRI analysis

UV-vis spectrophotometer (TU-1810, Purkinje, Beijing, China) was used to record absorption spectra using a 1-

cm quartz cuvette ranging from 200 to 800 nm (wavelength increment = 1 nm). Milli-Q water was used for the blank. Absorbance at 280 (A280) and specific ultraviolet absorbance at 254 nm (SUVA254), 260 nm (SUVA260), and 280 nm (SUVA280) were applied for the characterization of the optical properties. Specific ultraviolet absorbance (SUVA) is the ultraviolet absorbance of a sample at a given wavelength normalized for DOC concentration. And the specific ultraviolet absorbance at 254 nm (SUVA254), 260 nm (SUVA260), and 280 nm (SUVA280) was calculated by dividing the ultraviolet absorbance measured at $\lambda = 254$ nm, 260 nm, and 280 nm by the sample's DOC concentration (mg L^{-1}), respectively, expressed as liters per milligram per meter (Weishaar et al. 2003).

The EEM fluorescence spectra of the DOM were determined in a luminescence spectrometer (HITACHI F-4600). The excitation and emission wavelengths of fluorescence EEMs were 200 to 450 nm and 250 to 600 nm, respectively. Both excitation and emission were maintained at 5-nm intervals and the scanning speed was set at 1200 nm min^{-1} . To eliminate the water Raman scatter peaks, a Milli-Q water was used in the reference cell (Yu et al. 2019). The EEM spectra data was analyzed by FRI method to determine the fluorescence components. The calculation of the volume of each region was based on the Eq. (2) to Eq. (4):

$$\phi_i = \int_{\lambda_{\text{ex}}} \int_{\lambda_{\text{em}}} I(\lambda_{\text{ex}} \lambda_{\text{em}}) d\lambda_{\text{ex}} d\lambda_{\text{em}} \quad (2)$$

$$\Phi_{i,n} = MF_i \times \phi_i \quad (3)$$

$$\Phi T, n = \sum_{i=1}^5 \Phi_{i,n} \quad (4)$$

where φ_i is the volume of region i ($\text{au}\cdot\text{nm}^2$); λ_{ex} and λ_{em} are the fluorescence intensity in specific excitation wavelength and specific emission wavelength (au), respectively; MF_i is a multiplication factor.

Furthermore, the calculation of normalized excitation-emission area volume P_i was based on the Eq. (5):

$$P_{i,n} = \Phi_{i,n} / \Phi T, n \times 100\% \quad (5)$$

Estimation of the relative contribution

In this paper, the relative contributions of DOM source were estimated using the freeware package IsoSource. The software uses the isotope mass balance equation to calculate the proportions of the different end members of the mixture (Phillips et al. 2005). In this paper, the software was applied for the results from the isotope ratio and C/N.

Results and discussion

Distribution of $\delta^{13}\text{C}_{\text{DOM}}$ and C/N ratios of DOM and the relative contributions of sources at different sampling sites

Ranges of $\delta^{13}\text{C}_{\text{DOM}}$ and C/N ratios for Dagu River estuary are presented in Table 1 and Fig. 2. From the results, the $\delta^{13}\text{C}_{\text{DOM}}$ values of source samples are between -27.17 and -21.03‰ . The values of the aquaculture pond (-21.03‰) and farmland (-22.87‰) are the highest and the value of forest (-27.17‰) is the lowest. The $\delta^{13}\text{C}_{\text{DOM}}$ values of the surface sediment range from -20.93‰ (S8) to -26.55‰ (S9). Besides, the range of C/N value of the source samples is 7.12–14.17, with the industrial C/N (14.17) being the largest and the aquaculture pond C/N (7.12) being the lowest. The C/N values of surface sediment samples in downstream river are higher than those in the estuary, with the value of S3 as high as 10.30.

Figure 3 depicts the relative contributions of sources at nine sites. From the result, there are differences among relative contributions of sources. For S1, S2, S4, S5, and S8, the contributions of rural area and aquaculture pond have relatively high proportions. For S3, the relative contribution of industry (40%) is the highest. And farmland, rural area, and aquaculture contribute more than 10%, respectively. For S6, the relative contributions of forest, farmland, rural area, and aquaculture are greater than 15%. Similarly, forest, farmland, rural area, and aquaculture contribute more than 10% to S7, respectively. And S9 is characterized by industry whose relative contribution value is 93%. According to Regier et al. (2016),

Table 1 The values of $\delta^{13}\text{C}_{\text{DOM}}$ (‰) and C/N ratios for the samples of sources and sediments

	Samples	DOC (mg kg^{-1})	Stable isotope ratios	
			$\delta^{13}\text{C}$ (‰)	C/N
Source	Farmland	682.04 ± 39.43	-22.87	9.09 ± 0.7
	Forest	111.06 ± 7.68	-27.17	9.46 ± 0.47
	Industry	697.73 ± 38.68	-25.39	14.17 ± 0.06
	Aquaculture	1039.68 ± 11.74	-21.03	7.12 ± 0.79
	Rural area	872.05 ± 41.02	-24.31	7.33 ± 0.62
Sediment	S1	500.08 ± 11.74	-23.58	0.39 ± 0.07
	S2	412.24 ± 50.39	-22.92	3.56 ± 0.34
	S3	810.67 ± 24.70	-24.28	10.30 ± 0.48
	S4	205.18 ± 20.33	-24.83	3.34 ± 0.44
	S5	296.16 ± 43.70	-22.23	3.85 ± 0.64
	S6	562.82 ± 20.33	-24.58	8.80 ± 0.99
	S7	321.25 ± 54.52	-23.10	6.87 ± 0.35
	S8	989.49 ± 91.68	-20.93	6.11 ± 0.53
	S9	1077.33 ± 68.88	-26.55	21.10 ± 3.49

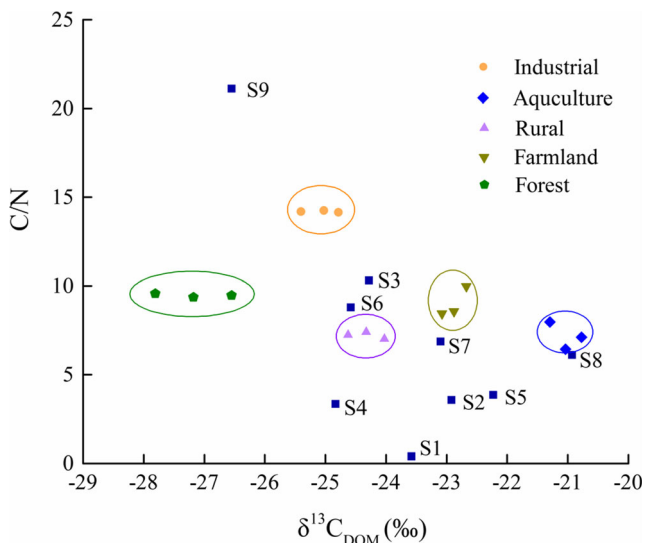


Fig. 2 The end-member plot of $\delta^{13}C_{DOM}$ versus C/N ratios for samples of sediments and sources

the runoff and surrounding land use have effects on the transportation of allochthonous DOM. Thus, the relative contribution of sources varies with the change of sites. Pollutants produced by rural area and aquaculture (which is mainly marine aquaculture including shellfish, shrimp, and other seafood)

contribute significantly to DOM sources; this is because in the past few decades, Dagu River estuary has been greatly influenced by the rapid population growth (Zhang et al. 2013; Liang et al. 2015). At S3 and S9 (i.e., large amounts of factories are distributed around S3 and S9), the industry has high relative contribution.

DOC contents and UV-vis absorption property

The DOC contents of sediment samples and source samples in Dagu River estuary are displayed in Table 1. The DOC contents in the surface sediment and source samples range from 205.18 to 1077.33 mg kg⁻¹ and 111.05 to 1024 mg kg⁻¹, with an average value of 575.02 and 680.51 mg kg⁻¹, respectively. The aquaculture pond has the highest DOC content among the source samples with the value of 1039.69 mg kg⁻¹ and the forest has the lowest DOC content of 111.06 mg kg⁻¹. The DOC contents of surface sediment at S9 and S8 are higher than those at S1 and S2, and the DOC contents of surface sediment at S5 and S4 are the lowest; this indicates that sediment DOC content in downstream river is higher than that in the estuary. The trend of DOC content in Dagu River estuary is similar to other river estuaries, with higher values of DOC

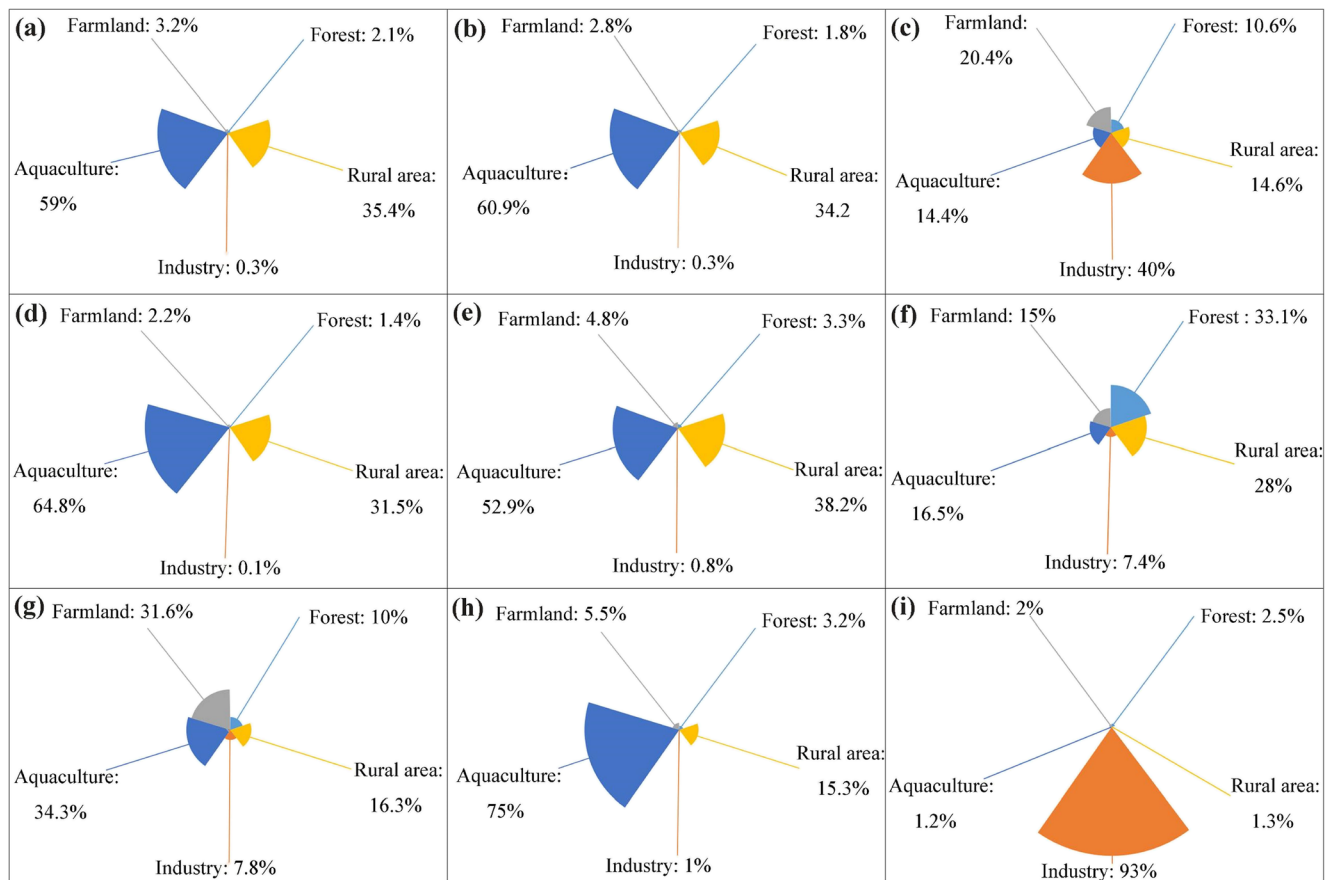


Fig. 3 The source contributions to sediments of nine sites. **a** S1, **b** S2, **c** S3, **d** S4, **e** S5, **f** S6, **g** S7, **h** S8, **i** S9

contents in the upstream freshwater than in coastal water (Asmala et al. 2013; Jiang et al. 2017). There are several explanations: (i) there are significant contributions from urban and industrial developments to DOM along the downstream river; (ii) high primary productivity in river increases the concentrations of DOC in river due to the activities of phytoplankton and zooplankton; (iii) riverine DOC contents gradually decrease because of biological and photochemical processes from downstream river to estuary of Dagū River. The result also shows that samples in the middle (S4–S7) have low DOC content, which would be caused by the dilution effects of tributaries and tidal backwater (Zhou et al. 2019).

In this study, we use SUVA254, SUVA260, A280, and SUVA280 value to investigate the characteristics of sediment DOM in Dagū River estuary. SUVA 254 value is widely used to indicate the abundance of aromatic carbon in DOM (Nishijima and Speitel 2004). The value of SUVA260 represents the content of hydrophobic fractions (Jaffrain et al. 2007). The absorption properties measured at 280 nm are correlated with molecular weight of aquatic natural organic matter (Leenheer and Croué 2003). Table 2 illustrates the values of nine sites. The ranges of SUVA254, SUVA260, and SUVA280 value of surface sediment samples are 0.18–1.23, 0.17–1.23, and 0.14–0.91 L mg⁻¹ m⁻¹, respectively. The A280 value of surface sediment samples varies from 0.07 to 0.63. From the result, the values of S9 are the largest among nine sites, and the values of S3 are the lowest. Moreover, the values of S9 are significantly higher than other sites, indicating the highest aromaticity, highest contents of hydrophobic fractions, and highest molecular weight of DOM at S9. It can be revealed that these UV absorption values have similar trend from the downstream river to the estuary. For example, there are higher values of the spectral parameters in downstream river than those in the estuary, demonstrating higher aromaticity, humification degree, contents of hydrophobic fractions, and molecular weight of DOM in the downstream river rather than in the estuary. According to Jiang et al. (2017), the lower UV absorption values of DOM in Dagū River estuary can be explained by two reasons: (i) highly humic and aromatic

components of DOM are removed due to the adsorption on suspended particulates; (ii) the estuary is more affected by marine DOM resulting in lower absorption, lower fluorescence, and lower DOC concentration than downstream river.

Fluorescence properties of DOM

Figure 4 illustrates the 3D-EEM fluorescence spectra of surface sediment DOM in Dagū River estuary. Five peaks can be detected from the fluorescence spectra. Peaks A and C are related to fulvic acid-like and humic acid-like compounds, respectively (Fu et al. 2005). Peak D is related to soluble microbial products. Peaks B and T belong to protein-like peaks. Each fluorescence spectra of DOM is classified into five regions based on the FRI theory as shown in Table 3 (Chen et al. 2003). For protein-like materials, regions I and II are mainly associated with tryptophan-like and tyrosine-like compounds, respectively (Chen et al. 2003). And region IV represents soluble microbial by-product substances (Wang et al. 2019). In addition, regions III and V are related to fulvic-like materials and humic-like materials (Chen et al. 2003). Besides, values of P_{i,n} for regions that represent the percentage fluorescence response in EEMs of DOM are calculated. The result suggests that the sources of DOM at 9 sites are different. This is mainly caused by the various human activities in surrounding area. In addition, according to Li et al. (2016), regions I and II are collectively classified as P(I+II, n); regions III and V are classified as P(III+V, n). From Fig. 5, the P(I+II, n) of sediment DOM ranges from 42.79 to 69.35%; P(IV, n) of DOM ranges from 6.97 to 10.69%. Moreover, the P(III+V, n) of DOM generally shows an increasing trend from S1 to S9, with values ranging from 23.59 to 47.50%.

The results exhibit that sediment DOM of S1–S5 mainly contains protein-like substances and few humic-like substances. The proportions of humic-like component and protein-like component are similar in the sediment DOM at S6 and S7. And there are more humic-like substances than protein-like substance in the sediment DOM at S8 and S9.

Table 2 UV-vis absorption spectra parameters (A280, SUVA280, SUVA254, and SUVA260) of sediment DOM

Sites	A280	SUVA280 (L mg ⁻¹ m ⁻¹)	SUVA254 (L mg ⁻¹ m ⁻¹)	SUVA260 (L mg ⁻¹ m ⁻¹)
S1	0.08	0.26	0.29	0.29
S2	0.1	0.38	0.45	0.44
S3	0.07	0.14	0.18	0.17
S4	0.07	0.56	0.65	0.64
S5	0.09	0.39	0.46	0.45
S6	0.1	0.27	0.31	0.3
S7	0.09	0.44	0.51	0.49
S8	0.23	0.37	0.47	0.46
S9	0.63	0.91	1.23	1.23

Table 3 Excitation and emitting (Ex/Em) wavelengths of fluorescence region (Yu et al. 2019)

Components	Fluorescence integral region		Fluorescence substance	Fluorescence peak	Fluorescence peak position	
	λ_{Ex} (nm)	λ_{Em} (nm)			λ_{Ex} (nm)	λ_{Em} (nm)
I	220~250	280~330	Tyrosine-like protein	B	220~230	300~310
II	220~250	330~380	Tryptophan-like protein	T	225~250	315~365
III	220~250	380~480	Fulvic acid-like organics	A	240~250	380~440
IV	250~360	280~380	Soluble microbial by-product	D	270~300	320~380
V	250~420	380~520	Humic acid-like organics	C	320~360	400~450

The percentage of humic-like substances decreases from downstream river to estuary, indicating that the degree of DOM humification in downstream river is higher than that in the estuary, which is in accordance with the result of UV-

vis spectra. The reason is that there are large amounts of villages and factories distributed in the downstream of Dagu River and the external DOM exports into Dagu River through runoff influencing DOM composition and altering its quality

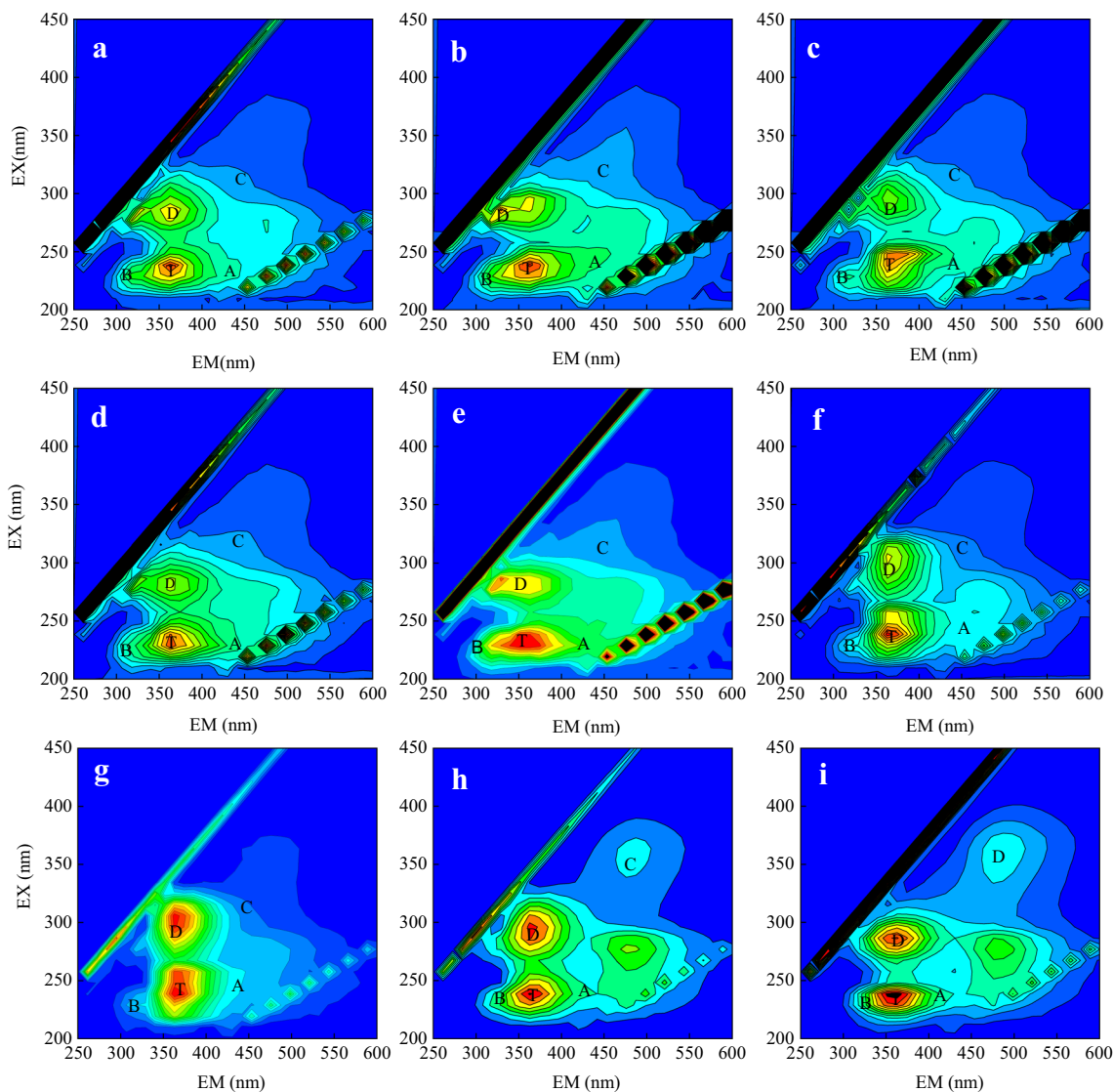
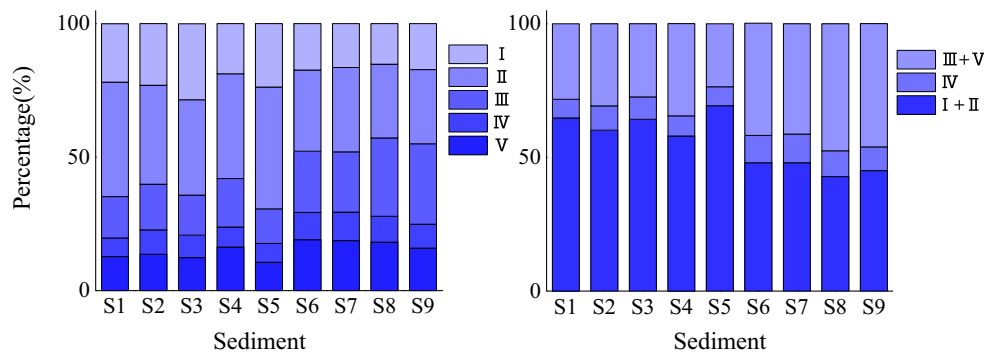


Fig. 4 Contour plots of five fluorescence components of DOM in sediment samples. (a) S1, (b) S2, (c) S3, (d) S4, (e) S5, (f) S6, (g) S7, (h) S8, (i) S9

Fig. 5 Percentage of fluorescence components of DOM in sediment



(Lu et al. 2016; Han et al. 2017; Wang et al. 2019). Thus, the humic-like substance content of sediment DOM in downstream river is higher than that in the estuary. Besides, according to Li et al. (2016), humic-like component can prevent excessive nutrients release. Thus, the result implies the release risk of nutrients in downstream river area would be lower than that in the estuary area.

Figure 6 illustrates the fluorescence parameters of sediment DOM. According to Wang et al. (2009), the fluorescence index (FI) can detect humic sources in DOM. The low FI value (1.4) indicates terrestrially derived humus components of DOM, and the high FI value (1.9) indicates microbially and/or algal-derived humus components of DOM (Wang et al. 2009). Figure 6 shows that the FI values of sediment DOM are in the range of 1.61–1.99 (the average value is 1.74) at different sites; this result implies that the DOM in Dagu River estuary sediments is influenced by terrestrial input and biological metabolism. It should be noted that FI values of some samples from downstream river sediment are slightly higher than 1.9. This is mainly because direct anthropogenic influences result in an increase of protein-like components (Jiang et al. 2017). For instance, excess nutrients from farmland

which is added with lots of fertilizers and wastewater from rural area may lead to higher production of autochthonous DOM in Dagu River.

The humification index (HIX) can indicate the degree of humification of organic matter (Hansen et al. 2016). High value of HIX suggests great humification of the source (Ohno 2002). Figure 6 shows that HIX values of sediment DOM in downstream river are higher than those in the estuary, indicating higher humification of sediment DOM in downstream river than that in the estuary. The trend of humification degree is in accordance with the result from SUVA₂₅₄ and FRI. Moreover, the biological/autochthonous index (BIX) is correlated to autochthonous DOM. High BIX value indicates high proportion of autochthonous DOM (Hansen et al. 2016). Figure 6 depicts that BIX values of DOM are in the range of 0.59–2.73 (the average value is 1.31) and BIX values of sediment DOM in downstream river are higher than those in the estuary on average. The result indicates that the sediment DOM in Dagu River estuary is influenced by both terrestrial input and biological metabolism.

The relationship between DOM characteristics and different forms of N and P contents in the sediment

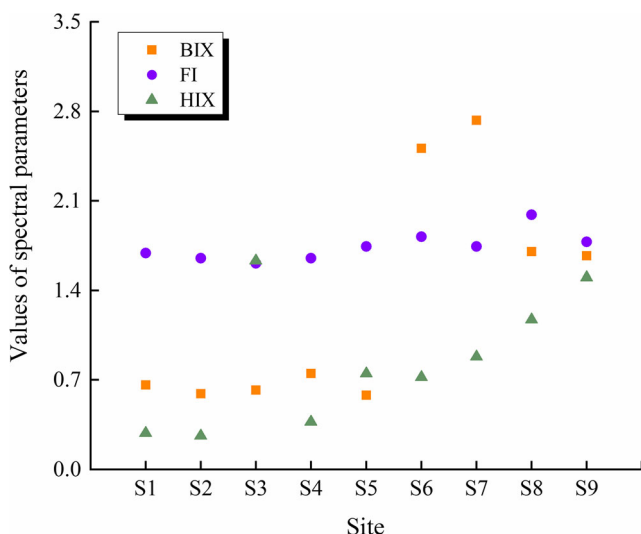


Fig. 6 Fluorescence parameters (HIX, BIX, and FI) values of DOM

The contents of different forms of N and P in the sediment were investigated (this can be seen in Table 4). From the result in Table 4, the ranges of $\text{NH}_4^+\text{-N}$, $\text{NO}_3^-\text{-N}$, TN, and AP contents are 3.21–18.83 mg kg^{-1} , 0.21–5.29 mg kg^{-1} , 19.65–51.31 mg kg^{-1} , and 8.18–17.37 mg kg^{-1} , respectively. And the contents of different forms of N and P in the sediment have a decrease trend from downstream river to the estuary. Table 5 illustrates the analysis of the correlation among the components of DOM and the contents of N and P in the sediments of Dagu River estuary. From the results in Table 5 and Fig. 7, the value of P(III,n) in the DOM sediment is positively correlated with the contents of TN and $\text{NH}_4^+\text{-N}$ in the sediment ($P < 0.05$). This result indicates that higher contents of TN and $\text{NH}_4^+\text{-N}$ are correlated with higher percentage of fulvic acid substances in DOM. In addition, there are significant positive correlations between the contents of $\text{NH}_4^+\text{-N}$ and the values of SUVA₂₅₄. The results suggest that

Table 4 Contents of different N and P forms in the surface sediments of Dagu river estuary (mg kg⁻¹)

Samples	NH ₄ ⁺ -N	NO ₃ ⁻ -N	TN	AP
S1	5.02 ± 0.08	0.52 ± 0.10	28.06 ± 0.46	8.69 ± 1.88
S2	6.2 ± 1.43	0.62 ± 0.13	34.85 ± 1.95	17.37 ± 3.57
S3	7.51 ± 0.54	0.21 ± 0.09	30.89 ± 1.55	8.18 ± 1.12
S4	5.18 ± 1.08	0.41 ± 0.03	30.58 ± 2.71	13.65 ± 0.54
S5	5.09 ± 0.53	4.26 ± 0.26	19.65 ± 3.56	8.84 ± 0.31
S6	4.76 ± 0.41	5.29 ± 0.35	29.07 ± 2.47	15.62 ± 1.93
S7	3.21 ± 0.17	4.19 ± 0.64	20.65 ± 2.58	10.15 ± 1.55
S8	12.47 ± 0.08	1.65 ± 0.21	49.80 ± 2.16	16.27 ± 1.61
S9	18.83 ± 2.27	1.34 ± 0.31	51.31 ± 7.11	10.22 ± 0.98

higher humification of DOM would result in higher NH₄⁺-N contents in the sediment. There are two reasons for these results: (i) humic-like substances can fix certain nutrients (polysaccharides and amino acids) and inhibit soil nitrification; (ii) humic-like substances can hinder the conversation of P by limiting the activity of alkaline phosphatase (Newman 1993). The results also imply that higher content of DOM significantly results in higher contents of TN and NH₄⁺-N. This is because DOM and nutrients (N and P) have a common origin. The contents of TN and NH₄⁺-N are positively correlated with the A280 of DOM. This would be related to the content of DOC.

Potential release risk assessment of heavy metals based on DOM characteristics

DOM can bind heavy metals, thereby decreasing the concentration of free metal ions in aquatic ecosystems, resulting in a reduction in the potential bioavailability of metal to aquatic organisms (Sánchez-Marín and Beiras 2012). Based on the

Table 5 Correlation coefficients between DOM characteristics and the content of N and P

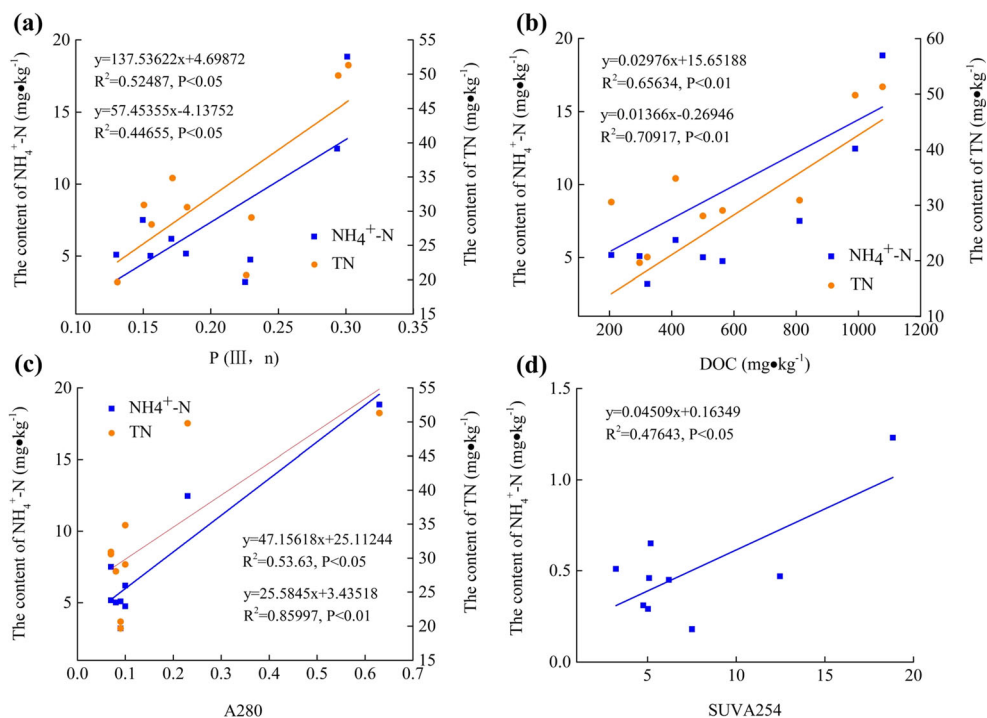
	AP	TN	NH ₄ ⁺ -N	NO ₃ ⁻ -N
DOC content	0.005	0.815**	0.863**	- 0.211
P(I,n)	- 0.434	- 0.384	- 0.279	- 0.394
P(II,n)	- 0.393	- 0.655	- 0.578	- 0.166
P(III,n)	0.36	0.761*	0.718*	0.152
P(IV,n)	0.458	0.213	0.098	0.472
P(V,n)	0.511	0.287	0.115	0.391
SUVA254	- 0.017	0.566	0.736*	- 0.14
A280	- 0.051	0.763*	0.937**	- 0.143

*Correlation is significant at the 0.05 level (2-tailed); **correlation is significant at the 0.01 level (2-tailed)

previous studies, the binding ability of DOM components and five heavy metals was sequenced and was assigned values based on the strength of combining ability. The combining ability between humic-like component and heavy metal follows the order of Cu > Pb > Zn > Cd > Hg (Tipping et al. 2011; Guo et al. 2012 ; Xu et al. 2013; Huang et al. 2018). And the binding ability of protein-like substances and heavy metal is in the order of Cu > Pb > Hg > Cd > Zn (Guo et al. 2012; Wu et al. 2012b; Xu et al. 2013; Huang et al. 2018). In addition, humus-like component exhibits higher Cu(II) and Pb(II) binding affinities than protein-like ones (Xu et al. 2019). As for Hg and Zn, the binding affinities with protein-like substances are higher than humus-like substances (Wufuer et al. 2014). Particularly, protein-like substances are the main fraction involved in Cd(II) complexation (Wu et al. 2012b). Considering the factors above, the widely used analytic hierarchy process (AHP) method was applied to investigate the weight of each type of combining ability (Sener and Davraz 2013). The weights of various complexation abilities were calculated. Weights of humus-like substance binding to Cu, Pb, Zn, Cd, and Hg are 0.2214, 0.1526, 0.0669, 0.0402, and 0.0188, respectively. And weights of protein-like substance binding to Cu, Pb, Zn, Cd, and Hg are 0.2066, 0.1013, 0.0235, 0.0430, and 0.1256, respectively. Thus, the ecological risks of single heavy metal in the sediment were calculated using equations in Appendix. The potential release risk values of heavy metals are represented in Table 6. For example, the potential release risk value of Cu varies from 2.38 to 12.42 of nine sites; the value range of Hg is 56.94–245.7. And the comprehensive ecological risk value ranges from 139.09 to 670.02. The result shows that the risk value of the middle zone is higher than that of the estuary and the downstream river.

In this study, the inverse distance weight (IDW) was applied to predict the potential ecological risk of heavy metal on the basis of consideration of data characteristics, research purpose, and sampling site. IDW is an interpolation method widely used to clarify the spatial variation and distribution of metals (Gu et al. 2012). From the results in Fig. 8, for Cu, Pb, Zn, and Cd in the sediment, the degree of ecological risks at S4 and S5 is higher than that at S2 and S1. And the degree of ecological risks at S8 and S9 is the lowest. The potential ecological risks of Hg at S4 are higher than those at other sites. The result indicates that for single heavy metal, the degree of ecological risk fluctuates at different sites, due to the different content and structural characteristics of sediment DOM at different sites. In general, the freshwater area has the lowest ecological risk. Samples in the middle transect have high potential ecological risks. The ranking of comprehensive ecological risk of heavy metals is similar to the ranking of single one. The result illustrates that the potential ecological risk of heavy metal in downstream river is lower than

Fig. 7 Relationships between $\text{NH}_4^+\text{-N}$, TN, and **a** P(III,n), **b** DOC, **c** A280, and **d** SUVA254 of sediment DOM in Dagu river estuary



that in the estuary. And samples in the middle transect (S4–S7) have high potential risks of heavy metal.

From all the results above, the humification degree of DOM is low and the potential risk of heavy metal release is high in the estuary where the relative contribution of aquaculture is high. The result is in accordance with that of Nimptsch et al. (2015), which suggested that DOM from land-based aquaculture is mainly consisted of protein-like substances. The result implies that (i) DOM from aquaculture sources might have high protein-like substance and (ii) DOM from aquaculture sources is related to high potential ecological risk of heavy metal release. It also shows that the protein-like proportion and the potential risk of heavy metal release would be higher when the relative contribution proportion of rural area increases. We cannot find relationship between farmland, forest, and DOM composition characteristics. This is due to the variation of agrotypes, soil type, farming intensive intensity, etc. (Fuß et al. 2017).

Conclusions

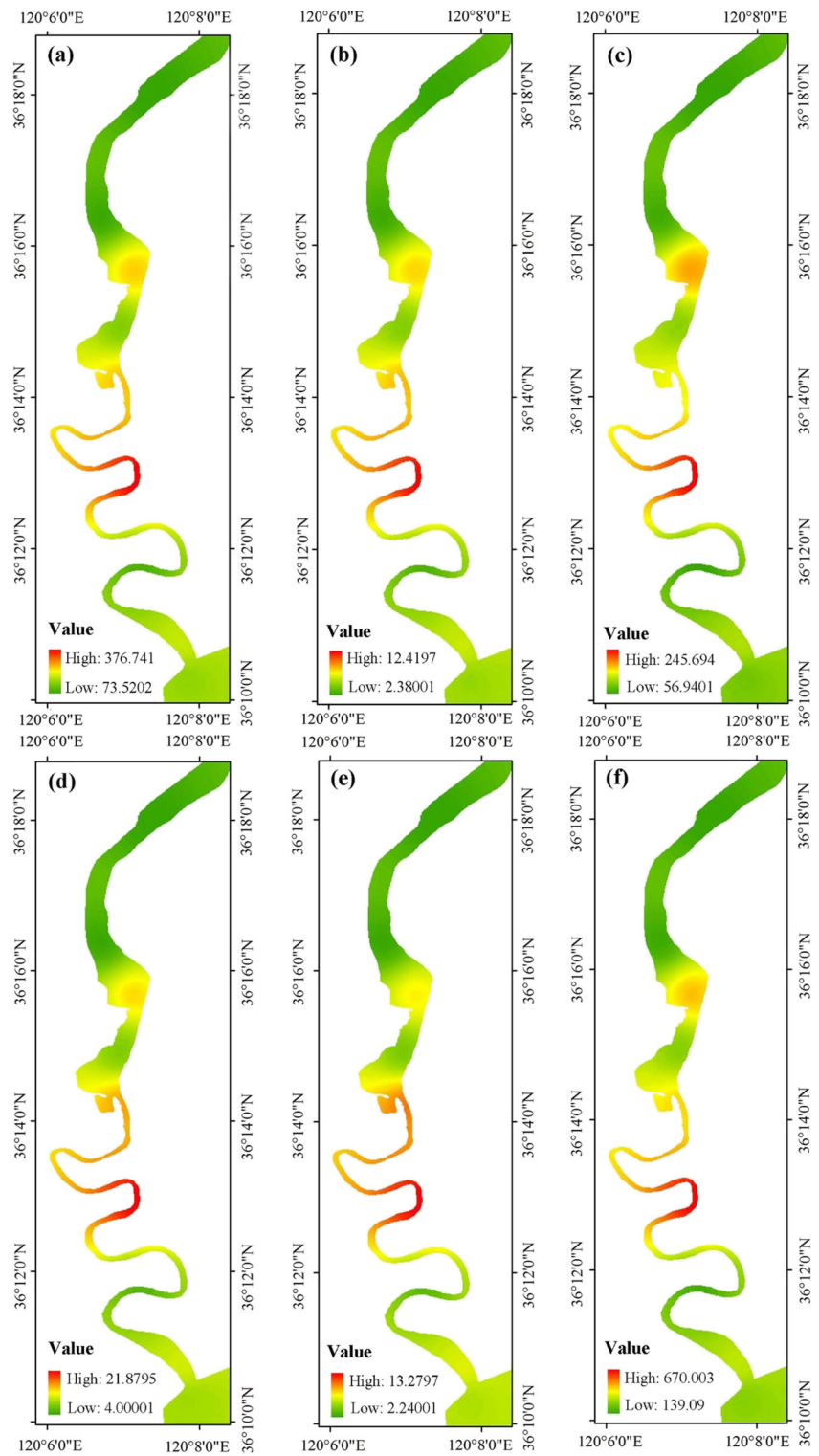
In this study, the sources, contents, and structural characteristics of Dagu River surface sediment DOM are revealed by carbon stable isotope ratios, C/N, UV-vis absorbance, and EEM spectroscopy, respectively. Then, the effect of content and structural characteristics of DOM on the content of different forms of N and P in the sediments is analyzed. Moreover, the potential release risks of heavy metals in the sediment at different sites are also evaluated. And some proper suggestions are proposed to direct human activities.

There are several discoveries: (i) rural area and aquaculture have great contributions to Dagu River estuary; (ii) the humification degree of DOM in downstream river is higher than that in the estuary; the composition of DOM in Dagu River estuary is affected by both terrestrial input and biological metabolism; (iii) the DOM in the sediment can reflect the potential risks of heavy metal release and eutrophication in the

Table 6 Potential ecological release risk values of heavy metal

Samples	Cu	Pb	Zn	Cd	Hg	Comprehensive ecological risk
S1	5.09	9.20	5.86	153.01	92.33	265.49
S2	6.31	11.25	6.99	190.39	119.29	334.23
S3	3.19	5.77	3.69	95.83	57.50	165.98
S4	12.42	21.88	13.28	376.75	245.70	670.02
S5	8.64	15.89	10.53	257.73	147.55	440.33
S6	4.63	7.89	4.52	142.13	104.26	263.42
S7	8.16	13.94	8.00	250.72	182.88	463.70
S8	2.61	4.36	2.42	80.86	64.50	154.75
S9	2.38	4.00	2.24	73.52	56.94	139.09

Fig. 8 Potential ecological release risk distributions of heavy metal in Dagu river estuary. **a** Cd, **b** Cu, **c** Hg, **d** Pb, **e** Zn, **f** comprehensive risk



estuary area. There is high potential risk of eutrophication in the estuary due to low humic-like substances in DOM; in addition, under the effect of aquaculture and rural area, there is higher potential ecological risk of heavy metal in the estuary than that in downstream river; samples in the middle transect

have the highest potential ecological risks of heavy metal. Therefore, the exogenous pollution (especially the rural area, industry, and aquaculture) should be controlled to decrease the potential risks of heavy metal and eutrophication, which are determined by the characteristics of DOM. In order to protect

the Dagu River estuary, the optimization and adjustment of rural area, industry, and aquaculture distributions are necessary to be improved.

There are still potential extensions: (i) we investigate the characteristics of sediment DOM in winter to indicate the ecological risk; it should be pointed out that the seasonal variation is an possible factor which influences DOM characteristics; the effects of different seasons on sediment DOM should be discussed in our future studies; (ii) we have not fully considered the impact of sea source in this paper; the influence of tidal on DOM content and structure characteristics in the estuary needs further study; (iii) our estimation of the ecological risk is not precise enough; more studies on quantitative assessment of the ecological risk in Dagu River estuary are desired in the future.

Funding information This work was supported by the National Natural Science Foundation of China (No. 41771098 and 51809145) and the Shandong Key Laboratory of Water Pollution Control and Resource Reuse (No. 2019KF10).

Appendix. The equation to calculate ecological risks of heavy metal in the sediment

The ecological risks of single heavy metal in the sediment ($R_{i,s}$) were calculated with equation (6):

$$R_{i,s} = T_i \times 1 / (A_s C_s) \quad (6)$$

The comprehensive ecological risk of heavy metals in the sediment (CR_s) at different sites were calculated with equation (7):

$$CR_s = \sum_{i=1}^n R_s \quad (7)$$

where C_s is the content of DOM at site s , A_s is the complexation ability at sites, and the biological toxicity factor (T_i) of heavy metal is as follows: Cu = Pb = Ni = 5, Cr = 2, Zn = 1, Pb = 5, Hg = 40, Cd = 30, As = 10, according to potential ecological risk index (PERI), which was established by Hakanson (1980).

References

- Asmala E, Autio R, Kaartokallio H, Pitkänen L, Stedmon CA, Thomas DN (2013) Bioavailability of riverine dissolved organic matter in three Baltic Sea estuaries and the effect of catchment land use. *Biogeosciences* 10:6969–6986. <https://doi.org/10.5194/bg-10-6969-2013>
- Boyes S, Elliott M (2006) Organic matter and nutrient inputs to the Humber Estuary, England. *Mar Pollut Bull* 53:136–143. <https://doi.org/10.1016/j.marpolbul.2005.09.011>
- Cao F, Tzortziou M, Hu C, Mannino A, Fichot CG, Vecchio RD, Najjar RG, Novak M (2018) Remote sensing retrievals of colored dissolved organic matter and dissolved organic carbon dynamics in north american estuaries and their margins. *Remote Sens Environ* 205:151–165
- Chen ML, Hur J (2015) Pre-treatments, characteristics, and biogeochemical dynamics of dissolved organic matter in sediments: a review. *Water Res* 79:10–25. <https://doi.org/10.1016/j.watres.2015.04.018>
- Chen W, Westerhoff P, Leenheer JA, Booksh K (2003) Fluorescence excitation-emission matrix regional integration to quantify spectra for dissolved organic matter. *Environ Sci Technol* 37:5701–5710. <https://doi.org/10.1021/es034354c>
- Chen ML, Kim SH, Jung HJ, Hyun JH, Choi JH, Lee HJ, Huh IA, Hur J (2017) Dynamics of dissolved organic matter in riverine sediments affected by weir impoundments: production, benthic flux, and environmental implications. *Water Res* 121:150–161. <https://doi.org/10.1016/j.watres.2017.05.022>
- Coble PG (1996) Characterization of marine and terrestrial DOM in seawater using excitation-emission matrix spectroscopy. *Mar Chem* 51:325–346. [https://doi.org/10.1016/0304-4203\(95\)00062-3](https://doi.org/10.1016/0304-4203(95)00062-3)
- Cong ZY, Kang SC, Kawamura K, Liu B, Xin W, Wang ZY, Gao SP, Fu PQ (2015) Carbonaceous aerosols on the south edge of the Tibetan Plateau: concentrations, seasonality and sources. *Atmos Chem Phys* 15:1573–1584. <https://doi.org/10.5194/acp-15-1573-2015>
- Dai JC, Song JM, Li XG, Yuan HM, Li N, Zheng GX (2007) Environmental changes reflected by sedimentary geochemistry in recent hundred years of Jiaozhou Bay, North China. *Environ Pollut* 145:656–667. <https://doi.org/10.1016/j.envpol.2006.10.005>
- Derrien M, Kim MS, Ock G, Hong S, Cho J, Shin KH, Hur J (2018) Estimation of different source contributions to sediment organic matter in an agricultural-forested watershed using end member mixing analyses based on stable isotope ratios and fluorescence spectroscopy. *Sci Total Environ* 618:569–578. <https://doi.org/10.1016/j.scitotenv.2017.11.067>
- Dong YR, Li Y, Kong FL, Zhang JL, Xi M (2020) Source, structural characteristics and ecological indication of dissolved organic matter extracted from sediments in the primary tributaries of the Dagu River. *Ecol Indic* 109:105776. <https://doi.org/10.1016/j.ecolind.2019.105776>
- Fu PQ, Liu CQ, Wu FC (2005) Study on the three-dimensional fluorescence spectra of dissolved organic matter. *Spectrosc Spectr Anal* 25:2024–2028
- Fuß T, Behounek B, Ulseth AJ, Singer GA (2017) Land use controls stream ecosystem metabolism by shifting dissolved organic matter and nutrient regimes. *Freshw Biol* 62:582–599. <https://doi.org/10.1111/fwb.12887>
- Gu Y, Wang Z, Lu S, Jiang S, Mu D, Shu Y (2012) Multivariate statistical and GIS-based approach to identify source of anthropogenic impacts on metallic elements in sediments from the mid Guangdong coasts, China. *Environ Pollut* 163:248–255. <https://doi.org/10.1016/j.envpol.2011.12.041>
- Guéguen C, Burns DC, McDonald A, Ring B (2012) Structural and optical characterization of dissolved organic matter from the lower Athabasca River, Canada. *Chemosphere* 87:932–937. <https://doi.org/10.1016/j.chemosphere.2012.01.047>
- Gul C, Praveen SP, Kang S, Adhikary B, Zhang YL, Ali S, Li Y, Li XF (2018) Concentrations and source regions of light absorbing impurities in snow/ice in northern Pakistan and their impact on snow albedo. *Atmos Chem Phys* 18:4981–5000. <https://doi.org/10.5194/acp-18-4981-2018>
- Guo XJ, Yuan DH, Li Q, Jiang JY, Chen FX, Zhang H (2012) Spectroscopic techniques for quantitative characterization of Cu(II) and Hg(II) complexation by dissolved organic matter from lake sediment in arid and semi-arid region. *Ecotoxicol Environ Saf* 85:144–150. <https://doi.org/10.1016/j.ecoenv.2012.08.016>

- Hakanson L (1980) An ecological risk index for aquatic pollution control: a sedimentological approach. *Water Res* 14:975–1001. [https://doi.org/10.1016/0043-1354\(80\)90143-8](https://doi.org/10.1016/0043-1354(80)90143-8)
- Han P, Li YX, Yang XF, Xue L, Zhang LJ (2017) Effects of aerobic respiration and nitrification on dissolved inorganic nitrogen and carbon dioxide in human-perturbed eastern Jiaozhou Bay, China. *Mar Pollut Bull* 124:449–458. <https://doi.org/10.1016/j.marpolbul.2017.07.055>
- Hansen AM, Kraus TEC, Pellerin BA, Fleck JA, Downing BD, Bergamaschi BA (2016) Optical properties of dissolved organic matter (DOM): Effects of biological and photolytic degradation. *Limnol Oceanogr* 61:1015–1032. <https://doi.org/10.1002/lno.10270>
- He XS, Xi BD, Wei ZM, Jiang YH, Geng CM, Yang Y, Yuan Y, Liu HL (2011) Physicochemical and spectroscopic characteristics of dissolved organic matter extracted from municipal solid waste (MSW) and their influence on the landfill biological stability. *Bioresour Technol* 102:2322–2327. <https://doi.org/10.1016/j.biortech.2010.10.085>
- He Y, Men B, Yang XF, Li YX, Xu H, Wang DS (2019) Relationship between heavy metals and dissolved organic matter released from sediment by bioturbation/bioirrigation. *J Environ Sci* 75:216–223 (in Chinese). <https://doi.org/10.1016/j.jes.2018.03.031>
- Hongve D (1999) Production of dissolved organic carbon in forested catchments. *J Hydrol* 224:91–99. [https://doi.org/10.1016/S0022-1694\(99\)00132-8](https://doi.org/10.1016/S0022-1694(99)00132-8)
- Huang M, Li ZW, Huang B, Luo NL, Zhang Q, Zhai XQ, Zeng GM (2018) Investigating binding characteristics of cadmium and copper to DOM derived from compost and rice straw using EEM-PARAFAC combined with two-dimensional FTIR correlation analyses. *J Hazard Mater* 344:539–548. <https://doi.org/10.1016/j.jhazmat.2017.10.022>
- Huguet A, Vacher L, Saubusse S, Etcheber H, Abril G, Relexans S, Ibalot F, Parlanti E (2010) New insights into the size distribution of fluorescent dissolved organic matter in estuarine waters. *Org Geochem* 41:595–610. <https://doi.org/10.1016/j.orggeochem.2010.02.006>
- Jaffrain J, Gerard F, Meyer M, Ranger J (2007) Assessing the quality of dissolved organic matter in forest soils using ultraviolet absorption spectrophotometry. *Soil Sci Soc Am J* 71:1851–1858. <https://doi.org/10.2136/sssaj2006.0202>
- Jahan S, Strezov V (2018) Comparison of pollution indices for the assessment of heavy metals in the sediments of seaports of NSW, Australia. *Mar Pollut Bull* 128:295–306. <https://doi.org/10.1016/j.marpolbul.2018.01.036>
- Ji ZM, Kang SC, Cong ZY, Zhang QG, Yao TD (2015) Simulation of carbonaceous aerosols over the Third Pole and adjacent regions: distribution, transportation, deposition, and climatic effects. *Clim Dyn* 45(9–10):2831–2846. <https://doi.org/10.1007/s00382-015-2509-1>
- Jiang X, Jin XC, Yao Y, Li LH, Wu FC (2008) Effects of biological activity, light, temperature and oxygen on phosphorus release processes at the sediment and water interface of Taihu Lake, China. *Water Res* 42:2251–2259. <https://doi.org/10.1016/j.watres.2007.12.003>
- Jiang T, Skyllberg U, Björn E, Green NW, Tang JH, Wang DY, Gao J, Li CX (2017) Characteristics of dissolved organic matter (DOM) and relationship with dissolved mercury in Xiaoqing River-Laizhou Bay estuary, Bohai Sea, China. *Environ Pollut* 223:19–30. <https://doi.org/10.1016/j.envpol.2016.12.006>
- Kang SC, Zhang QG, Qian Y, Ji ZM, Li CL, Cong ZY, Zhang YL, Guo JM, Du WT, Huang J, You QL, Panday A, Rupakheti M, Chen DL, Gustafsson Ö, Thiemens MH, Qin DH (2019) Linking atmospheric pollution to cryospheric change in the Third Pole Region: current progresses and future prospects. *Nat Sci Rev* nwz031. <https://doi.org/10.1093/nsr/nwz031>
- Leenheer JA, Croué J (2003) Characterizing dissolved aquatic organic matter. *Environ Sci Technol* 1:19–26. <https://doi.org/10.1021/es032333c>
- Li YP, Wang SR, Zhang L, Zhao HC, Jiao LX, Zhao YL, He XS (2014) Composition and spectroscopic characteristics of dissolved organic matter extracted from the sediment of Erhai Lake in China. *J Soils Sediments* 14:1599–1611. <https://doi.org/10.1007/s11368-014-0916-2>
- Li P, Chen L, Zhang W, Huang Q (2015) Spatiotemporal distribution, sources, and photobleaching imprint of dissolved organic matter in the Yangtze Estuary and its adjacent sea using fluorescence and parallel factor analysis. *PLoS One* 10:e0130852. <https://doi.org/10.1371/journal.pone.0130852>
- Li YP, Zhang L, Wang SR, Zhao HC, Zhang R (2016) Composition, structural characteristics and indication of water quality of dissolved organic matter in Dongting Lake sediments. *Ecol Eng* 97:370–380. <https://doi.org/10.1016/j.ecoleng.2016.10.035>
- Liang SK, Pearson S, Wu W, Ma YJ, Qiao LL, Wang XH, Li JM, Wang XL (2015) Research and integrated coastal zone management in rapidly developing estuarine harbours: a review to inform sustainment of functions in Jiaozhou Bay, China. *Ocean Coast Manag* 116:470–477. <https://doi.org/10.1016/j.ocecoaman.2015.09.014>
- Liu JN, Du JZ, Wu Y, Liu SM (2018) Nutrient input through submarine groundwater discharge in two major Chinese estuaries: the Pearl River Estuary and the Changjiang River Estuary. *Estuar Coast Shelf Sci* 203:17–28. <https://doi.org/10.1016/j.ecss.2018.02.005>
- Liu C, Li ZW, Berhe AA, Xiao HB, Liu L, Wang DY, Peng H, Zeng GM (2019) Characterizing dissolved organic matter in eroded sediments from a loess hilly catchment using fluorescence EEM-PARAFAC and UV-visible absorption: insights from source identification and carbon cycling. *Geoderma* 334:37–48. <https://doi.org/10.1016/j.geoderma.2018.07.029>
- Louis Y, Pernet-Coudrier B, Varrault G (2014) Implications of effluent organic matter and its hydrophilic fraction on zinc(II) complexation in rivers under strong urban pressure: aromaticity as an inaccurate indicator of DOM-metal binding. *Sci Total Environ* 490:830–837. <https://doi.org/10.1016/j.scitotenv.2014.04.123>
- Lu DL, Yang NN, Liang SK, Li KQ, Wang XL (2016) Comparison of land-based sources with ambient estuarine concentrations of total dissolved nitrogen in Jiaozhou Bay (China). *Estuar Coast Shelf Sci* 180:82–90. <https://doi.org/10.1016/j.ecss.2016.06.032>
- McKnight DM, Boyer EW, Westerhoff PK, Doran PT, Kulbe T, Andersen DT (2001) Spectrofluorometric characterization of dissolved organic matter for indication of precursor organic material and aromaticity. *Limnol Oceanogr* 46:38–48. <https://doi.org/10.4319/lo.2001.46.1.0038>
- Meng FG, Huang GC, Yang X, Li ZQ, Li J, Cao J, Wang ZJ, Sun L (2013) Identifying the sources and fate of anthropogenically impacted dissolved organic matter (DOM) in urbanized rivers. *Water Res* 47:5027–5039. <https://doi.org/10.1016/j.watres.2013.05.043>
- Newman SA (1993) Phosphatase activity in the sediment-water column at a hypereutrophic lake. *J Environ Qual* 22:832–838
- Nimptsch J, Woelfl S, Osorio S, Valenzuela J, Ebersbach P, Tuempling W, Palma R, Encina F, Figueroa D, Kamjunke N, Graeber D (2015) Tracing dissolved organic matter (DOM) from land-based aquaculture systems in North Patagonian streams. *Sci Total Environ* 537: 129–138. <https://doi.org/10.1016/j.scitotenv.2015.07.160>
- Nishijima W, Speitel GE (2004) Fate of biodegradable dissolved organic carbon produced by ozonation on biological activated carbon. *Chemosphere* 56:113–119. <https://doi.org/10.1016/j.chemosphere.2004.03.009>
- Niu HW, Kang SC, Shi XF, He YQ, Lu XX (2017) Water-soluble elements in snow and ice on Mt. Yulong. *Sci Total Environ* 574:889–900. <https://doi.org/10.1016/j.scitotenv.2016.09.114>
- Niu HW, Kang SC, Wang HL, Zhang RD, Lu XX, Qian Y, Paudyal R, Wang SJ, Shi XF, Yan X (2018) Spatio-temporal variability and light absorption property of carbonaceous aerosol in a typical glacier

- region of the southeastern Tibetan Plateau. *Atmos Chem Phys* 18:1–19
- Ohno T (2002) Fluorescence inner-filtering correction for determining the humification index of dissolved organic matter. *Environ Sci Technol* 36:742–746. <https://doi.org/10.1021/es0155276>
- Omar TFT, Aris AZ, Yusoff FD, Mustafa S (2018) Occurrence, distribution, and sources of emerging organic contaminants in tropical coastal sediments of anthropogenically impacted Klang River estuary, Malaysia. *Mar Pollut Bull* 131:284–293. <https://doi.org/10.1016/j.marpolbul.2018.04.019>
- Phillips DL, Newsome SD, Gregg JW (2005) Combining sources in stable isotope mixing models: alternative methods. *Oecologia* 144: 520–527. <https://doi.org/10.1007/s00442-004-1816-8>
- Regier P, Briceño H, Jaffé R (2016) Long-term environmental drivers of DOC fluxes: linkages between management, hydrology and climate in a subtropical coastal estuary. *Estuar Coast Shelf Sci* 182:112–122. <https://doi.org/10.1016/j.ecss.2016.09.017>
- Sánchez-Marín P, Beiras R (2012) Quantification of the increase in Pb bioavailability to marine organisms caused by different types of DOM from terrestrial and river origin. *Aquat Toxicol* 110–111:45–53. <https://doi.org/10.1016/j.aquatox.2011.12.015>
- Sellami F, Hachicha S, Chtourou M, Medhioub K, Ammar E (2008) Maturity assessment of composted olive mill wastes using UV spectra and humification parameters. *Bioresour Technol* 99:6900–6907. <https://doi.org/10.1016/j.biortech.2008.01.055>
- Sener E, Davraz A (2013) Assessment of groundwater vulnerability based on a modified DRASTIC Model, GIS and an Analytic Hierarchy Process (AHP) method: the case of Egridir Lake Basin (Isparta, Turkey). *J Hydrol* 21:701–714. <https://doi.org/10.1007/s10040-012-0947-y>
- Shang P, Lu YH, Du YX, Jaffé R, Findlay RH, Wynn A (2018) Climatic and watershed controls of dissolved organic matter variation in streams across a gradient of agricultural land use. *Sci Total Environ* 612:1442–1453. <https://doi.org/10.1016/j.scitotenv.2017.08.322>
- Tian W, Li LZ, Liu F (2012) Assessment of the maturity and biological parameters of compost produced from dairy manure and rice chaff by excitation-emission matrix fluorescence spectroscopy. *Bioresour Technol* 110:330–337. <https://doi.org/10.1016/j.biortech.2012.01.067>
- Tipping E, Lofts S, Sonke JE (2011) Humic ion-binding model VII: a revised parameterisation of cation-binding by humic substances. *Environ Chem* 8:225–235. <https://doi.org/10.1071/EN11016>
- Wang ZW, Wu ZC, Tang SJ (2009) Characterization of dissolved organic matter in a submerged membrane bioreactor by using three-dimensional excitation and emission matrix fluorescence spectroscopy. *Water Res* 43:1533–1540. <https://doi.org/10.1016/j.watres.2008.12.033>
- Wang Y, Zhang D, Shen ZY, Feng CH, Zhang X (2015) Investigation of the interaction between As and Sb species and dissolved organic matter in the Yangtze Estuary, China, using excitation-emission matrices with parallel factor analysis. *Environ Sci Pollut Res* 22: 1819–1830. <https://doi.org/10.1007/s11356-014-3380-z>
- Wang YL, Hu YY, Yang CM, Wang QJ, Jiang DG (2019) Variations of DOM quantity and compositions along WWTPs-river-lake continuum: implications for watershed environmental management. *Chemosphere* 218:468–476. <https://doi.org/10.1016/j.chemosphere.2018.11.037>
- Weishaar JL, Aiken GR, Bergamaschi BA, Fram SM, Fujii R, Mopper K (2003) Evaluation of specific ultraviolet absorbance as an indicator of the chemical composition and reactivity of dissolved organic carbon. *Environ Sci Technol* 37:4702–4708. <https://doi.org/10.1021/es030360x>
- Wu DD, Ge CD, Gao S, Lu YM, Yang Y (2012a) Carbon, nitrogen geochemical character and source analyse in Changjiang estuarine sediments. *Geochimica* 41:207–215. <https://doi.org/10.1007/s11783-011-0280-z>
- Wu J, Zhang H, Yao QS, Shao LM, He PJ (2012b) Toward understanding the role of individual fluorescent components in DOM-metal binding. *J Hazard Mater* 215–216:294–301. <https://doi.org/10.1016/j.jhazmat.2012.02.075>
- Wufuer R, Liu Y, Mu SY, Song WJ, Yang X, Zhang DY, Pan XL (2014) Interaction of dissolved organic matter with Hg(II) along salinity gradient in boston lake. *Geochem Int* + 52: 1072–1077. <https://doi.org/10.1134/s001670291412009x>
- Xi M, Kong FL, Li Y, Kong FT (2017) Temporal-spatial variation of DOC concentration, UV absorbance and the flux estimation in the Lower Dagou River, China. *Front Earth Sci* 11:660–669. <https://doi.org/10.1007/s11707-017-0633-4>
- Xi M, Zi YY, Wang QG, Wang S, Cui GL, Kong FL (2018) Assessment of the content, structure, and source of soil dissolved organic matter in the coastal wetlands of Jiaozhou Bay, China. *Phys Chem Earth* 103:35–44. <https://doi.org/10.1016/j.pce.2017.03.004>
- Xie H, Aubry C, Bélanger S, Song G (2012) The dynamics of absorption coefficients of CDOM and particles in the St. Lawrence estuarine system: biogeochemical and physical implications. *Mar Chem* 128–129:44–56. <https://doi.org/10.1016/j.marchem.2011.10.001>
- Xie MW, Chen M, Wang WX (2018) Spatial and temporal variations of bulk and colloidal dissolved organic matter in a large anthropogenically perturbed estuary. *Environ Pollut* 243:1528–1538. <https://doi.org/10.1016/j.envpol.2018.09.119>
- Xu HC, Yu GH, Yang LY, Jiang HL (2013) Combination of two-dimensional correlation spectroscopy and parallel factor analysis to characterize the binding of heavy metals with DOM in lake sediments. *J Hazard Mater* 263:412–421. <https://doi.org/10.1016/j.jhazmat.2013.09.042>
- Xu HC, Zou L, Guan DX, Li WT, Jiang HL (2019) Molecular weight-dependent spectral and metal binding properties of sediment dissolved organic matter from different origins. *Sci Total Environ* 665:828–835. <https://doi.org/10.1016/j.scitotenv.2019.02.186>
- Yu X, Zhang JL, Kong FL, Li Y, Li MM, Dong YR, Xi M (2019) Identification of source apportionment and its spatial variability of dissolved organic matter in Dagou River-Jiaozhou Bay estuary based on the isotope and fluorescence spectroscopy analysis. *Ecol Indic* 102:528–537. <https://doi.org/10.1016/j.ecolind.2019.03.004>
- Zhang YP, Yang GP, Lu XL, Ding HB, Zhang HH (2013) Distributions of dissolved monosaccharides and polysaccharides in the surface microlayer and surface water of the Jiaozhou Bay and its adjacent area. *Cont Shelf Res* 63:85–93
- Zhang JL, Li YP, Zeng XT, Huang GH, Li Y, Zhu Y, Kong FL, Xi M, Liu J (2019) Effluent trading planning and its application in water quality management: a factor-interaction perspective. *Environ Res* 168:286–305. <https://doi.org/10.1016/j.envres.2018.09.029>
- Zhang JL, Wang X, Sun WN, Li YP, Liu ZR, Liu YR, Huang GH (2020) Application of fiducial method for streamflow prediction under small sample cases in Xiangxihe watershed, China. *J Hydrol* 586: 124866. <https://doi.org/10.1016/j.jhydrol.2020.124866>
- Zhou YQ, Li Y, Yao XL, Ding WH, Zhang YB, Jeppesen E, Zhang YL, Podgorski DC, Chen CM, Ding Y, Wu HW, Spencer RGM (2019) Response of chromophoric dissolved organic matter dynamics to tidal oscillations and anthropogenic disturbances in a large subtropical estuary. *Sci Total Environ* 662:769–778. <https://doi.org/10.1016/j.scitotenv.2019.01.220>
- Zhu MK, Kong FL, Li Y, Li MM, Zhang JL, Xi M (2020) Effects of moisture and salinity on soil dissolved organic matter and ecological risk of coastal wetland. *Environ Res* 187:109659. <https://doi.org/10.1016/j.envres.2020.109659>

Publisher's note Springer Nature remains neutral with regard to jurisdictional claims in published maps and institutional affiliations.